



# Toxin $\zeta$ Triggers a Survival Response to Cope with Stress and Persistence

María Moreno-del Álamo, Mariangela Tabone <sup>†</sup>, Virginia S. Lioy <sup>†</sup> and Juan C. Alonso <sup>\*</sup>

Department of Microbial Biotechnology, Centro Nacional de Biotecnología (CSIC), Madrid, Spain

## OPEN ACCESS

### Edited by:

Manuel Espinosa,  
Centro de Investigaciones Biológicas  
(CSIC), Spain

### Reviewed by:

Ramon Diaz Orejas,  
Consejo Superior de Investigaciones  
Científicas (CSIC), Spain  
Nadia Berkova,  
Institut National de la Recherche  
Agronomique (INRA), France

### \*Correspondence:

Juan C. Alonso  
jcalonso@cnb.csic.es

### <sup>†</sup>Present Address:

Mariangela Tabone,  
Department of Basic Biomedical  
Sciences, Faculty of Biomedical  
Sciences and Health, Universidad  
Europea de Madrid, Madrid, Spain;  
Virginia S. Lioy,  
Institute for Integrative Biology of the  
Cell (I2BC), CEA, Centre National de la  
Recherche Scientifique, Univ.  
Paris-Sud, Université Paris-Saclay,  
Gif-sur-Yvette, France.

### Specialty section:

This article was submitted to  
Evolutionary and Genomic  
Microbiology,  
a section of the journal  
Frontiers in Microbiology

**Received:** 17 April 2017

**Accepted:** 02 June 2017

**Published:** 23 June 2017

### Citation:

Moreno-del Álamo M, Tabone M,  
Lioy VS and Alonso JC (2017) Toxin  $\zeta$   
Triggers a Survival Response to Cope  
with Stress and Persistence.  
*Front. Microbiol.* 8:1130.  
doi: 10.3389/fmicb.2017.01130

Bacteria have evolved complex regulatory controls in response to various environmental stresses. Protein toxins of the  $\zeta$  superfamily, found in prominent human pathogens, are broadly distributed in nature. We show that  $\zeta$  is a uridine diphosphate-N-acetylglucosamine (UNAG)-dependent ATPase whose activity is inhibited *in vitro* by stoichiometric concentrations of  $\epsilon_2$  antitoxin. *In vivo*, transient  $\zeta$  expression promotes a reversible multi-level response by altering the pool of signaling purine nucleotides, which leads to growth arrest (dormancy), although a small cell subpopulation persists rather than tolerating toxin action. High c-di-AMP levels (absence of phosphodiesterase GdpP) decrease, and low c-di-AMP levels (absence of diadenylate cyclase DisA) increase the rate of  $\zeta$  persistence. The absence of CodY, a transition regulator from exponential to stationary phase, sensitizes cells to toxin action, and suppresses persisters formed in the  $\Delta disA$  context. These changes, which do not affect the levels of stochastic ampicillin (Amp) persistence, sensitize cells to toxin and Amp action. Our findings provide an explanation for the connection between  $\zeta$ -mediated growth arrest (with alterations in the GTP and c-di-AMP pools) and persistence formation.

**Keywords:** toxin-antitoxin system, cell wall inhibition, c-di-AMP, CodY, (p)ppGpp, DisA

## INTRODUCTION

The toxin-antitoxin (TA) systems are widely distributed in free-living bacteria, in their extrachromosomal elements, and in archaea (Gerdes, 2013; Unterholzner et al., 2013). The toxins of all known TA systems are proteins while the antitoxins are either proteins or non-coding RNAs. The TA systems are classified into five different TA types (Yamaguchi et al., 2011), being the most broadly distributed the type II TA system, where both the toxin and the antitoxin are proteins (Leplae et al., 2011; Gerdes, 2013). The type II toxins use different strategies to regulate growth control and cellular processes related to the general stress response. Toxins of the  $\zeta$ /PezT superfamily, which are among the most broadly distributed in nature, are found in major human pathogens and in environmentally important bacteria of the phylum Firmicutes (Mutschler and Meinhart, 2013). The plasmid-borne  $\zeta$  gene product from *Streptococcus pyogenes*, *Streptococcus agalactiae* or *Enterococcus faecalis* and the chromosome-encoded  $\zeta$  toxin from *Clostridium perfringens* or *Staphylococcus aureus* (~285 amino acids) share ~43% sequence identity with chromosome-encoded *Streptococcus pneumoniae* or *Streptococcus suis* PezT toxin (~255 amino acids) (reviewed in Mutschler and Meinhart, 2013). When free in solution, these toxins interact with uridine diphosphate-N-acetylglucosamine (UNAG), ATP-Mg<sup>2+</sup> or GTP-Mg<sup>2+</sup> (denoted ATP and GTP), and with their cognate dimeric  $\epsilon$ /PezA antitoxin ( $\epsilon$ /PezA<sub>2</sub>) (Meinhart et al., 2001, 2003; Khoo et al., 2007; Mutschler et al., 2011). A non-toxic heterotetrameric complex

( $\zeta\epsilon_2\zeta$ /PezT-PezA<sub>2</sub>-PezT) interacts with UNAG, but not with ATP/GTP (Meinhart et al., 2001, 2003; Khoo et al., 2007; Mutschler et al., 2011).

Enzymes of the  $\zeta$ /PezT toxin superfamily have a common fold core with phosphotransferases (Meinhart et al., 2001, 2003; Khoo et al., 2007; Mutschler et al., 2011). Toxin  $\zeta$ /PezT transfers the ATP/GTP  $\gamma$ -phosphate to the 3'-hydroxyl group of the UNAG amino sugar, rendering UNAG-3P unreactive and thus reducing cell wall biosynthesis (Mutschler et al., 2011). Although, a quantitative analysis of this reaction showed that in the presence of limiting UNAG and ATP, toxin  $\zeta$  mainly hydrolyzed ATP and only traces of the  $\gamma$ -phosphate are transferred to UNAG (Tabone et al., 2014a).

The fine mechanisms of bacterial responses to toxin action are not generally conserved among different bacterial phyla (Gerdes, 2013). The evolutionary distance between *Escherichia coli* and *Bacillus subtilis*, which is larger than the time divergence between yeasts and humans, reflects the notable differences made by the purine nucleotides in the stringent response (Potrykus and Cashel, 2008; Liu et al., 2015). In *E. coli* (a representative of the  $\gamma$ -proteobacteria class), toxin-mediated persister formation is linked to high levels of guanosine (penta)tetraphosphate ([p]ppGpp), which inhibits the PPX phosphatase; dropping of PPX increases polyphosphate levels that activate Lon protease degradation of the antitoxins, with subsequent release of active toxins (Maisonneuve et al., 2013). These free mRNAse toxins contribute to persistence to some, but not all antibiotics (Harms et al., 2016). The role of toxin action in bacteria of the phylum Firmicutes, and whether these toxins induce persistence or tolerance, is poorly understood. We therefore examined the role of *S. pyogenes* pSM19035-encoded  $\zeta$  toxin in growth arrest (dormancy), alone or with antibiotic in *B. subtilis* cells (representative of the Firmicutes), by controlling expression of the toxin at or near physiological concentrations. In our analysis, we did not study the role of (p)ppGpp in antitoxin degradation and free toxin release. We found that transient expression of a short-lived toxin  $\zeta$  variant ( $\zeta$ Y83C) induced different temporal sets of cell responses and growth arrest, but a small cell subpopulation ( $5 \times 10^{-5}$  to  $1 \times 10^{-4}$ ) exits the dormant state, leading to persistent or tolerant *B. subtilis* cells (Lioy et al., 2012).

Analysis of the metabolic changes induced by the free toxin showed that within the first 5 min,  $\zeta$ Y83C expression decreased the intracellular GTP pool and dysregulated transcription of 78 genes, of which 28 with reduced expression are essential for cell proliferation (Lioy et al., 2012). Induction of genes involved in the SOS response was not observed, but the expression was documented of genes that could modulate toxin action, such as increased *comGA* and *relA* expression or decreased *glmS* gene expression (Lioy et al., 2012). It is likely that by altering ATP:GTP ratios, toxin  $\zeta$ Y83C modifies availability of the initiating nucleotides; this in turn changes promoter preferences by RNA polymerase, and the intracellular signaling (Krasny and Gourse, 2004; Pedley and Benkovic, 2017).

Within the first 15 min of  $\zeta$ Y83C expression, the intracellular ATP concentration decreases and that of (p)ppGpp increases (Lioy et al., 2012). The contribution of increased *comGA* and *relA*

expression lead to higher (p)ppGpp levels (Potrykus and Cashel, 2008; Hahn et al., 2015; Liu et al., 2015), which directly inhibit both salvage and *de novo* GTP synthesis (Lopez et al., 1981; Kriel et al., 2012; Pedley and Benkovic, 2017). In *B. subtilis*, low GTP levels lead to derepression of CodY, a global transcriptional regulator from exponential to stationary phase (Handke et al., 2008; Kriel et al., 2012; Bittner et al., 2014; Brinsmade et al., 2014).

Downregulation of *GlmS* contributes indirectly to reducing the pool of UNAG synthesis, and a small UNAG pool increases levels of the essential cyclic 3,5-diadenosine monophosphate (c-di-AMP) second messenger (Witte et al., 2008; Zhu et al., 2016). Changes in the intracellular level of c-di-AMP, which play an essential role in K<sup>+</sup> transport and cell wall homeostasis (Gundlach et al., 2017), indirectly increase the intracellular (p)ppGpp pool (Rao et al., 2010; Corrigan et al., 2015). The relationship between the effective levels of c-di-AMP and bacterial persisters is nonetheless poorly characterized.

At later stages of toxin  $\zeta$ Y83C expression, synthesis of macromolecules (DNA, RNA, proteins) is inhibited and membrane potential is impaired (30–90 min; Lioy et al., 2012). Direct interaction of (p)ppGpp with DNA primase inhibits DNA replication (Wang et al., 2007; Srivatsan and Wang, 2008), (p)ppGpp-mediated low levels of GTP decrease mRNA transcription (Krasny and Gourse, 2004), and the essential GTPases decrease the amount of mature 70S ribosomes and reduce translation (Corrigan et al., 2016). Within 60–120 min, cell wall biosynthesis is reduced by  $\zeta$ -mediated phosphorylation of a UNAG fraction, leading to accumulation of unreactive UNAG-3P (Mutschler et al., 2011; Lioy et al., 2012), and by (p)ppGpp inhibition of peptidoglycan metabolism (Eymann et al., 2002). All these metabolic changes are reversible, however, because when the stress condition is relieved (or after artificial induction of antitoxin expression), the antitoxin  $\epsilon_2$  reverses the  $\zeta$ -induced dormant state and the cell population “awakens” (Tabone et al., 2014a,b).

When bacterial growth is challenged by addition of antibiotic, susceptible cells stop growing, but a small subpopulation shows persistence (a biphasic time-inactivation curve) or tolerance to the drug (a linear time-inactivation curve; see **Figure 1**; Lewis, 2010; Amato et al., 2013; Brauner et al., 2016). These complex phenotypes have been attributed to diverse stochastically induced stresses, with the toxin reducing the activity of the antibiotic or enhancing efflux activities to form persisters or tolerant cells (Lewis, 2010; Balaban et al., 2013; Brauner et al., 2016; Harms et al., 2016) or to produce cells susceptible to antibiotic action, as in *B. subtilis* (Wu et al., 2011; Tabone et al., 2014b). Toxin  $\zeta$  increases (p)ppGpp and decreases GTP pools, thus decreasing antibiotic persistence/tolerance formation; in contrast, low, dysregulated (p)ppGpp levels (in the  $\Delta$ *relA* context) increase toxin and antibiotic persistence/tolerance (Tabone et al., 2014b).

To analyze how toxin  $\zeta$  helps to induce a growth arrest state (dormancy), how antitoxin  $\epsilon_2$  promotes exit from this state, and to learn about the interconnection between toxin action and the persister/tolerant state, we have studied the metabolic activities of purine nucleotides on persister/tolerant bacterial. Transient controlled expression experiments with toxin and antitoxin showed that toxin  $\zeta$  induced a reversible growth-arrested state

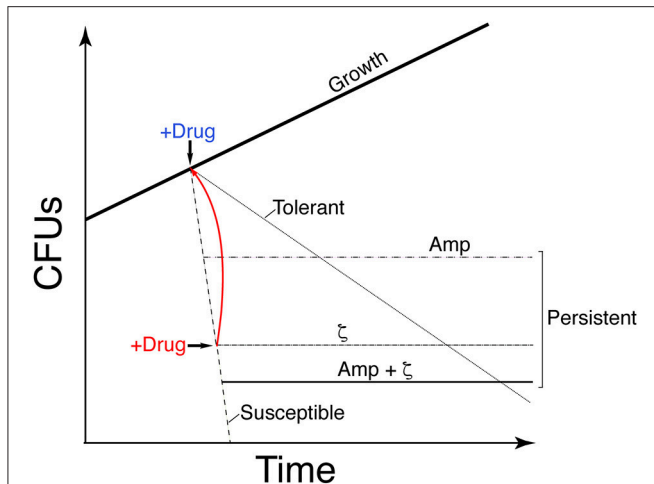


**FIGURE 1** | Graphic illustration showing the difference in growth of the different stress survival strategies. Proliferation of susceptible clonal cells is halted by transient toxin  $\zeta$  expression (IPTG addition) or Amp addition (2x MIC) (+Drug, blue). A large fraction of cells is susceptible to the drug (dashed line); a subpopulation persists and forms colonies, leading to a biphasic time-inactivation curve ( $\zeta$  [dotdashed] or Amp [twodotted dashed] persisters) rather than a linear time-inactivation curve (tolerants; dotted line). Transient expression of antitoxin  $\varepsilon_2$  (+Drug, red) awakens the susceptible cells to toxin  $\zeta$  action (solid red line). Transient toxin  $\zeta$  expression and Amp addition yield distinct persister subpopulations.

in a large fraction of proliferating, susceptible *B. subtilis* cells, but that a small subpopulation persists rather than tolerating toxin action (see **Figure 1**). Controlled upregulation of antitoxin  $\varepsilon_2$  reversed growth arrest *in vivo* and inhibited the UNAG-dependent ATPase activity of toxin  $\zeta$  *in vitro*. GdpP- or DisA-dependent alteration of the c-di-AMP pool and CodY-dependent responses revealed that ampicillin (Amp) persisters and  $\zeta$ -mediated persisters are distinct subpopulations, perhaps with different exit control, and that Amp enhanced killing of  $\zeta$ -mediated persisters.

## MATERIALS AND METHODS

### Bacterial Strains and Plasmids

The bacterial strains and plasmids used in this study are listed in **Table 1**. All *B. subtilis* strains are isogenic with BG214. *Escherichia coli* BL21(DE3) cells harboring pBT290-borne  $\varepsilon$  gene under the transcriptional control of the T7 RNA polymerase-dependent promoter ( $P_{T7}$ ), or pCB920-borne wild type (*wt*)  $\zeta$  gene under the control of  $P_{T7}$  and  $\varepsilon$  gene under its native RNA polymerase  $\sigma^A$ -dependent promoter ( $P_\omega$ ) were used for protein purification as described (Camacho et al., 2002; Tabone et al., 2014b).

### Growth Conditions

The BG214 derivatives were grown to mid-exponential phase ( $\sim 5 \times 10^7$  cells  $\text{ml}^{-1}$ ) at  $37^\circ\text{C}$  in minimal medium S7 (MMS7) supplemented with the necessary amino acid (Lioy et al., 2006). Except for  $\Delta relA$ , strains were grown in MMS7 with methionine and tryptophan at  $50 \mu\text{g ml}^{-1}$  each (Lioy et al., 2006). The  $\Delta relA$

**TABLE 1** | Bacterial strains.

| Strains                | Relevant genotype  | References           |
|------------------------|--|----------------------|
| BG1125 <sup>a,b</sup>  | + <i>lacI</i> , $P_{hsp}$ $\zeta$ , <i>aadA</i> [pCB799- <i>xylR</i> , $P_{xylA}$ $\varepsilon$ , <i>cat</i> ] | Lioy et al., 2006    |
| BG689 <sup>a</sup>     | + <i>xylR</i> , $P_{xylA}$ $\zeta$ Y83C, <i>cat</i>  | Lioy et al., 2006    |
| BG1145 <sup>a</sup>    | + $\Delta relA$ , <i>xylR</i> , $P_{xylA}$ $\zeta$ Y83C, <i>cat</i>  | Lioy et al., 2012    |
| BG1325 <sup>a</sup>    | + $\Delta gdpP$ , <i>xylR</i> , $P_{xylA}$ $\zeta$ Y83C, <i>cat</i>  | This study           |
| BG1323 <sup>a</sup>    | + $\Delta disA$ , <i>xylR</i> , $P_{xylA}$ $\zeta$ Y83C, <i>cat</i>  | This study           |
| BG1525 <sup>a</sup>    | + <i>codY::(erm::spc)</i> , <i>xylR</i> , $P_{xylA}$ $\zeta$ Y83C, <i>cat</i>                                  | This study           |
| BG1527 <sup>a</sup>    | + <i>codY::(erm::spc)</i> , $\Delta disA$ , <i>xylR</i> , $P_{xylA}$ $\zeta$ Y83C, <i>cat</i>                  | This study           |
| BL21(DE3) <sup>c</sup> | + [pCB920, $P_{T7}$ $\zeta$ gene, $P_\omega$ $\omega$ and $\varepsilon$ genes, <i>bla</i> ]                    | Tabone et al., 2014a |
| BL21(DE3) <sup>c</sup> | + [pBT290, $P_{T7}$ $\varepsilon$ gene, <i>bla</i> ]   | Camacho et al., 2002 |

<sup>a</sup>All *Bacillus subtilis* strains are isogenic with BG214 (*trpCE metA5 amyE1 ytsJ1 rsbV37 xre1 xkdA1 att<sup>SPB</sup> att<sup>CEBs1</sup>*).

<sup>b</sup>BG1125 cells bearing pCB799-borne  $\varepsilon$  gene were grown in MMS7 medium containing 0.05% xylose to titrate basal expression of the *wt*  $\zeta$  toxin.

<sup>c</sup>*Escherichia coli* BL21(DE3) genotype (*ompT gal [λ. DE3, int::lacI::Plac<sub>UV5</sub>::T7 gene 1] fruA2 [dcm] ΔhdsS*).

strain shows an “auxotrophy phenotype” for valine, leucine, isoleucine and threonine, and was also supplemented with these amino acids ( $25 \mu\text{g ml}^{-1}$  each) (Roche, Germany; Lioy et al., 2006).

BG1125 bearing *lacI*- $P_{hsp}$  *wt*  $\zeta$  and pCB799-borne *xylR*- $P_{xylA}$  *wt*  $\varepsilon$  (**Table 1**), in which  $\zeta$  gene expression (transcribed by  $P_{hsp}$ ) is regulated by IPTG (Calbiochem, Spain) addition and the  $\varepsilon$  gene (transcribed by  $P_{xylA}$ ) is regulated by xylose (Xyl, Sigma, USA) addition (Lioy et al., 2012), was grown in MMS7 supplemented with Xyl (0.05%). In the absence of IPTG [Sigma, USA] there are  $\sim 40$   $\zeta$  toxin monomers/colony-forming units (CFU), which lead to genetic rearrangement. To titrate basal  $\zeta$  toxin levels, traces of Xyl (0.05%) were added to allow synthesis of low but marked  $\varepsilon_2$  antitoxin levels by the pCB799-borne  $\varepsilon$  gene. After IPTG addition, toxin  $\zeta$  concentration increased in a very short time (10 min) up to  $\sim 1,500$   $\zeta$  monomers/CFU, and its steady-state level remained for at least 240 min; these toxin levels are considered the “physiological concentration” (Lioy et al., 2012). At indicated times, 0.5% Xyl was added to induce antitoxin  $\varepsilon_2$  expression, and the culture was incubated 15 min before being plated without inductor or with 0.5% Xyl (Lioy et al., 2012).

In BG689 or BG1145 bearing the *xylR*- $P_{xylA}$   $\zeta$ Y83C cassette (**Table 1**), expression of the toxin  $\zeta$ Y83C variant was induced by addition of 0.5% Xyl. BG689 or BG1145 cells were grown in MMS7 to  $\sim 5 \times 10^7$  cells  $\text{ml}^{-1}$  at  $37^\circ\text{C}$ . Xylose addition increased  $\zeta$ Y83C levels to a plateau within the first 10 min, and the steady-state level of the toxin remained for at least 240 min (Tabone et al., 2014b).

Where indicated, toxin and/or antitoxin expression was induced by adding IPTG and/or Xyl. Before plating, cells were centrifuged and resuspended in fresh LB medium to remove the inductor or the antibiotic, and dilutions were plated on LB agar plates containing glucose (which switches off *xylR*- $P_{xylA}$  cassette expression) or Xyl to express the  $\varepsilon_2$  antitoxin. The

survival rate was derived from the number of CFU in a given condition relative to CFU of the non-induced/non-antibiotic-treated control. Except  $\Delta relA$ , cells grew in MMS7 with a doubling time of 50–60 min. The doubling time of  $\Delta relA$  cells increased 1.4-fold compared to the BG689 strain. Normal-sized and small colonies were observed in the  $\Delta relA$  and  $\Delta disA codY$  contexts. All plates were incubated for 20 h at 37°C.

The minimum inhibitory concentration (MIC) of Amp [Sigma, USA] was estimated by exposing  $1-3 \times 10^6$  cells  $ml^{-1}$  (16 h, 37°C) in MMS7 with shaking (240 rpm). The Amp concentration used ( $3 \mu g ml^{-1}$ ) was twice the MIC (2x MIC). In the absence of inducer, the presence of the  $\zeta Y83C$  (BG689 strain) or the  $\zeta$  gene (BG1125 bearing pCB799) does not affect the MIC (Tabone et al., 2014b).

## Protein Purification and Biochemical Assays

The *S. pyogenes* pSM19035-encoded  $\zeta$  gene was overexpressed in *E. coli* BL21(DE3) cells from a rifampicin-resistant T7 RNAP-dependent promoter as reported (Tabone et al., 2014a). In short, IPTG was added to induce the expression of T7 RNAP that transcribed *wt*  $\zeta$  toxin, and 30 min later rifampicin (Fluka, USA), was added to selectively block the expression of the  $\omega$  and  $\epsilon$  genes. After 120 min of incubation and full decay of the  $\epsilon_2$  antitoxin, the cells were harvested. The over-expressed long-living  $\zeta$  toxin was purified in two steps as described (Tabone et al., 2014a). The fractions containing the  $\zeta$  protein were dialyzed against buffer A (50 mM Tris-HCl pH 7.5, 80 mM NaCl) containing 50% glycerol and stored at  $-20^\circ C$ . The  $\epsilon$  gene was overexpressed in *E. coli* BL21(DE3) cells harboring pBT290 under the control of rifampicin-resistant  $P_{T7}$  (Ceglowski et al., 1993), and antitoxin  $\epsilon_2$  was overexpressed, and purified as described (Camacho et al., 2002). The purified protein was stored in buffer A containing 50% glycerol at  $-20^\circ C$  (Camacho et al., 2002).

The ATPase, dATPase or GTPase activities of  $\zeta$  toxin were measured using a (d)NTP/NADH-linked assay (De La Cruz et al., 2000; Yadav et al., 2012). Reactions (50  $\mu l$ ) contained the indicated concentration of  $\zeta$  toxin and the NADH enzyme mix (310  $\mu M$  NADH [Roche, Germany], 100 U  $ml^{-1}$  lactic dehydrogenase [Sigma, USA], 500 U  $ml^{-1}$  pyruvate kinase [Roche, Germany], and 2.5 mM phosphoenolpyruvate [Roche, Germany]) in buffer B (50 mM Tris-HCl pH 7.5, 50 mM NaCl, 10 mM MgOAc, 1 mM DTT, 50  $\mu g/ml$  BSA) with the indicated concentration of ATP, GTP or dATP, and 10 mM UNAG or uridine diphosphate-N-acetylgalactosamine (UNAGal) [Sigma, USA]. We determined the specific (d)NTPase activity (in  $\mu M$ ) by measuring the (d)NDP production rate using a Shimadzu CPS-20A dual-beam spectrophotometer as described (Yadav et al., 2012). A standard curve with known amounts of NADH was obtained and used to convert the rate of ADP/GDP/dADP production from absorbance/time to concentration/rate (De La Cruz et al., 2000; Yadav et al., 2012).

## RESULTS

### Toxin $\zeta$ Preferentially Hydrolyzes ATP

Toxin  $\zeta$  hydrolyzes ATP, even in the presence of a 10- to 15-fold excess of cold GTP (Tabone et al., 2014a), suggesting that

toxin  $\zeta$  prefers ATP to GTP (Tabone et al., 2014a). To examine these reactions, we purified toxin  $\zeta$  in the absence of its cognate antitoxin  $\epsilon_2$ .

In the absence of UNAG, toxin  $\zeta$  does not undergo autophosphorylation or hydrolyze NTP; with UNAG (2 mM) and 500 nM toxin  $\zeta$ , only traces of the  $\gamma$ -phosphate of ATP (0.5 mM) were transferred to UNAG (Tabone et al., 2014a). We tested directly for nucleotide used preferentially by toxin  $\zeta$ . Limiting  $\zeta$  concentrations (60 nM) were used to analyze  $\zeta$ -mediated ATP, GTP or dATP hydrolysis in physiological concentrations of UNAG and of nucleotides. The *B. subtilis* intracellular UNAG, ATP, GTP, and dATP pools approached  $\sim 10$ ,  $\sim 10$ ,  $\sim 5$  and  $\sim 0.02$  mM, respectively (Lopez et al., 1979; Liroy et al., 2012; Bittner et al., 2014).

Toxin  $\zeta$  did not hydrolyze purine nucleotide when UNAG was omitted (Figure 2A). At physiological UNAG and ATP concentrations (10 mM each), toxin  $\zeta$  (60 nM) hydrolyzed ATP in a reaction that rapidly reached saturation, which suggested that  $\zeta$  is a UNAG-dependent NTPase. The final rate of  $\zeta$  ATP hydrolysis approached the maximum rate ( $K_{cat}$ ) of  $1520 \pm 120 \text{ min}^{-1}$  (Figure 2A).

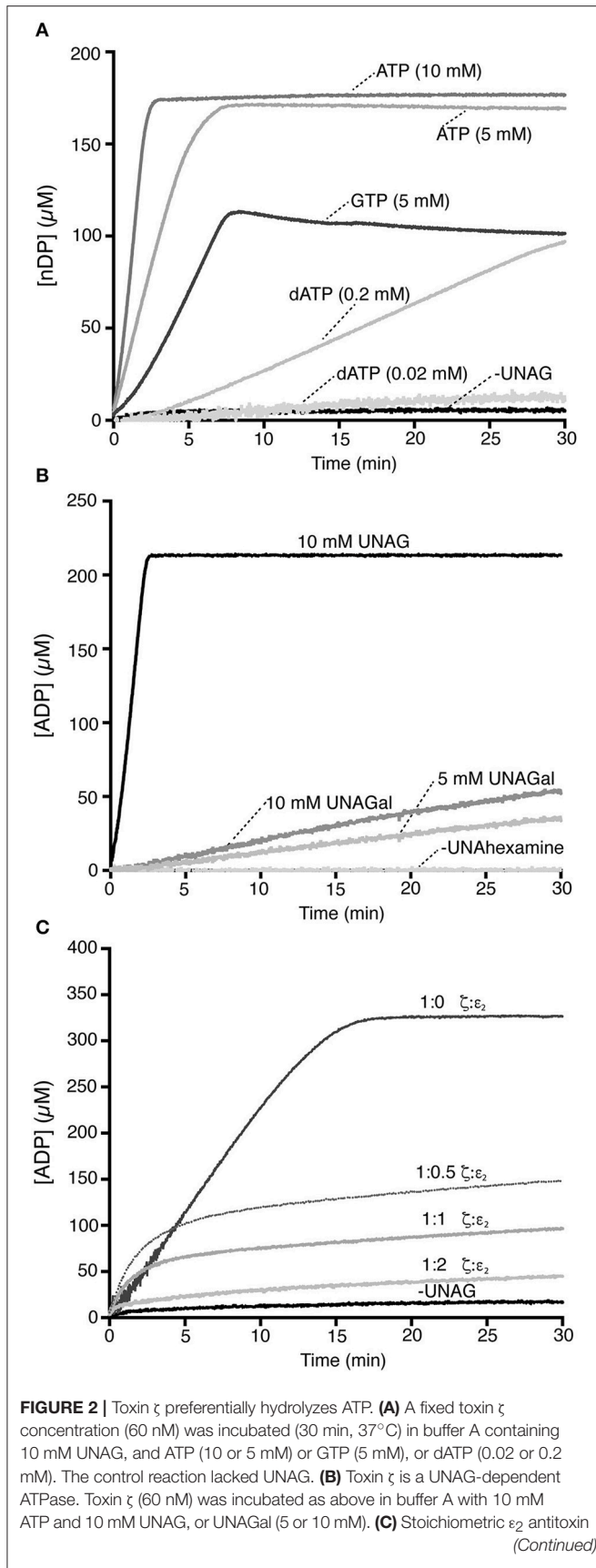
The UNAG-dependent  $\zeta$  ATPase activity was then compared with a *bona fide* ATPase enzyme. When the single-stranded DNA-dependent RecA ATPase was measured in parallel, *B. subtilis* RecA hydrolyzed ATP at near the previously observed  $K_{cat}$  of  $9 \pm 0.3 \text{ min}^{-1}$  (Yadav et al., 2014; Carrasco et al., 2015), which suggested that  $\zeta$  is a very robust ATPase. UNAG-dependent  $\zeta$ -mediated ATP hydrolysis was nonetheless sensitive to variations in ATP concentration, because when ATP was reduced to half (5 mM), the  $K_{cat}$  was reduced  $\sim 3$ -fold ( $510 \pm 44 \text{ min}^{-1}$ ).

When ATP was replaced by physiological GTP concentrations (5 mM),  $\zeta$  was able to hydrolyze GTP in a UNAG-dependent manner and the reaction reached saturation in  $\sim 7$  min. The final steady state rate of GTP hydrolysis was reduced by  $\sim 5$ -fold ( $K_{cat} 280 \pm 47 \text{ min}^{-1}$ ) compared with physiological ATP concentrations (Figure 2A). Increasing the GTP concentration to 10 mM did not improve the reaction.

We analyzed the potential role of dATP as a substrate (Figure 2A). In the presence of physiological UNAG and dATP concentrations (10 and 0.02 mM, respectively), we observed no  $\zeta$ -mediated UNAG-dependent dATP hydrolysis (Figure 2A). To test whether  $\zeta$  catalyzes dATP hydrolysis, we increased its concentration artificially. At a 10-fold excess of dATP (0.2 mM),  $\sim 3$  min lag time was needed to reach the steady state rate of  $\zeta$ -mediated dATP hydrolysis; however, saturation was not reached in 30 min reaction (Figure 2A). With a 10-fold excess of dATP, its hydrolysis was reduced by  $\sim 20$ -fold compared with ATP. ATP is probably the preferred  $\zeta$  nucleotide cofactor.

### UNAGal Is a Poor Inducer of the Toxin $\zeta$ ATPase

Toxin  $\zeta$  interacts specifically with UNAG rather than UDP-glucose (Mutschler et al., 2011); in addition, *B. subtilis* GalE is able to interconvert UNAG and UDP-N-acetylgalactosamine (UNAGal), and the cell wall contains N-acetylglucosamine and N-acetylgalactosamine (Soldo et al., 2003). To determine whether UNAGal, a C-4 epimer of UNAG, can activate toxin  $\zeta$  ATPase

**FIGURE 2 |** Continued

inhibits the UNAG-dependent  $\zeta$  ATPase. A fixed  $\zeta$  toxin concentration (30 nM) and increasing antitoxin  $\epsilon_2$  concentrations (15–60 nM) were incubated (30 min, 37°C) in buffer A containing limiting concentrations of ATP (2 mM) and UNAG (4 mM). The amount of ATP hydrolyzed was calculated (see Section Materials and Methods). The control reaction lacks UNAG. All reactions were repeated three or more times with similar results.

activity, we carried out ATPase assays with increasing UNAGal concentrations.

In the absence of UNAG or UNAGal (minus UNAhexamines), ATP hydrolysis by toxin  $\zeta$  was at background level (**Figure 2B**). Quantitative analysis of these reactions showed that at physiological UNAGal concentrations, the final  $\zeta$ -mediated ATP hydrolysis rate was  $\sim 85$ -fold lower ( $K_{cat}$  20  $\text{min}^{-1}$ ) than  $\zeta$  in the presence of UNAG. In the presence of a UNAGal excess (10 mM), the  $K_{cat}$  was slightly increased (28  $\text{min}^{-1}$ ), but was still  $\sim 60$ -fold lower than that at physiological UNAG concentrations (**Figure 2B**); this result indicates that  $\zeta$  ATPase activity is specifically stimulated by UNAG rather than by UNAGal. PetZ similarly accumulates UNAG-3P after 60 min, and UNAGal-3P after 720 min incubation (Mutschler et al., 2011).

### Antitoxin $\epsilon_2$ Inhibits UNAG-Dependent $\zeta$ -Mediated ATP Hydrolysis

*In vitro*, the  $\zeta\epsilon_2\zeta$  complex is reported to hydrolyze ATP and phosphorylate UNAG to form inactive UNAG-3P (Mutschler et al., 2011). In contrast, *in vivo* experiments showed that the  $\epsilon_2$  antitoxin inhibits the effect of toxin  $\zeta$ , perhaps by forming the inactive  $\zeta\epsilon_2\zeta$  complex (Lioy et al., 2006, 2010). To test whether toxin  $\zeta$  hydrolyzes ATP in the presence of the antitoxin  $\epsilon_2$ , both proteins were purified separately (Camacho et al., 2002; Tabone et al., 2014a) and UNAG-dependent ATPase activity measured.

The antitoxin  $\epsilon_2$ , alone or with UNAG, did not hydrolyze ATP (**Figure 2C**). In the presence of UNAG and ATP, the rate of UNAG-dependent  $\zeta$ -mediated ATP hydrolysis was reduced by increasing antitoxin  $\epsilon_2$  concentrations (**Figure 2C**). At  $\zeta:\epsilon_2$  ratios of 1:0.5 or 1:1, the kinetics of  $\zeta$ -mediated ATP hydrolysis was initially unaltered, but ATP hydrolysis was inhibited after 5 min. At a slight  $\epsilon_2$  excess (1:2 ratio), the antitoxin inhibited  $\zeta$  ATPase activity (**Figure 2C**). Results were similar when both proteins were preincubated (5 min) at a 1:1  $\zeta:\epsilon_2$  ratio ( $\zeta\epsilon_2\zeta$  complex; not shown), which suggests that when it interacts with  $\zeta$ , the antitoxin occupies the ATP binding pocket (Meinhart et al., 2003) and inhibits toxin ATPase activity. This is consistent with the crystal structure of the biologically inactive  $\zeta\epsilon_2\zeta$  complex and with the interpretation that antitoxin  $\epsilon_2$  is necessary and sufficient to inactivate toxin  $\zeta$ . It is likely that the long reaction incubation time (24 h) and/or low  $\epsilon_2$  stability could explain discrepancies with the previous report (Mutschler et al., 2011).

### Toxin $\zeta$ Induces Reversible Growth Arrest But a Small Subpopulation Evades Its Action

The release of toxins from their cognate antitoxins [or induction of toxin expression (+Drug in blue in **Figure 1**)], should lead

to a bimodal time-inactivation curve if persisters appeared (dotdashed line). This deviates from the simple decay, anticipated for a population of only susceptible cells (dashed line) or for a uniformly tolerant bacterial population (dotted line, in **Figure 1**; Brauner et al., 2016; Harms et al., 2016). Inactivation of the toxin by expression of the antitoxin (+Drug in red) should lead to recovery of the plating efficiency (red solid line) if the toxin is bacteriostatic (**Figure 1**). To test whether expression of physiological levels of free toxin  $\zeta$  induce persistence (dotdashed line) or tolerance (dotted line) and to study the mechanism used for such a phenotype (bacteriostasis or bacteriolysis) we performed long term survival assays. Toxin  $\zeta$  was induced for a long period, and then antitoxin  $\varepsilon_2$  expression was induced (**Figure 3A**).

*Bacillus subtilis* BG1125 bearing the  $\zeta$  gene under the control of IPTG induction is prone to rearrangement in the absence of IPTG (Lioy et al., 2012). To overcome this effect, the pCB799-borne  $\varepsilon$  gene under the control of Xyl was transferred into the background (**Table 1**; see Section Materials and Methods). BG1125 cells bearing pCB799 were grown in MMS7 supplemented with 0.05% Xyl, to  $\sim 5 \times 10^7$  cells  $\text{ml}^{-1}$  ( $\text{OD}_{560} = 0.2$ ), and expression of the  $\zeta$  gene was induced by IPTG addition (time zero). Cells, which formed colonies after plating on LB agar without IPTG, showed a bimodal time-inactivation curve suggesting the presence of persisters (**Figure 3A**), rather than showing a uniform simple decay, expected for tolerant cells (**Figure 1**, dotted line).

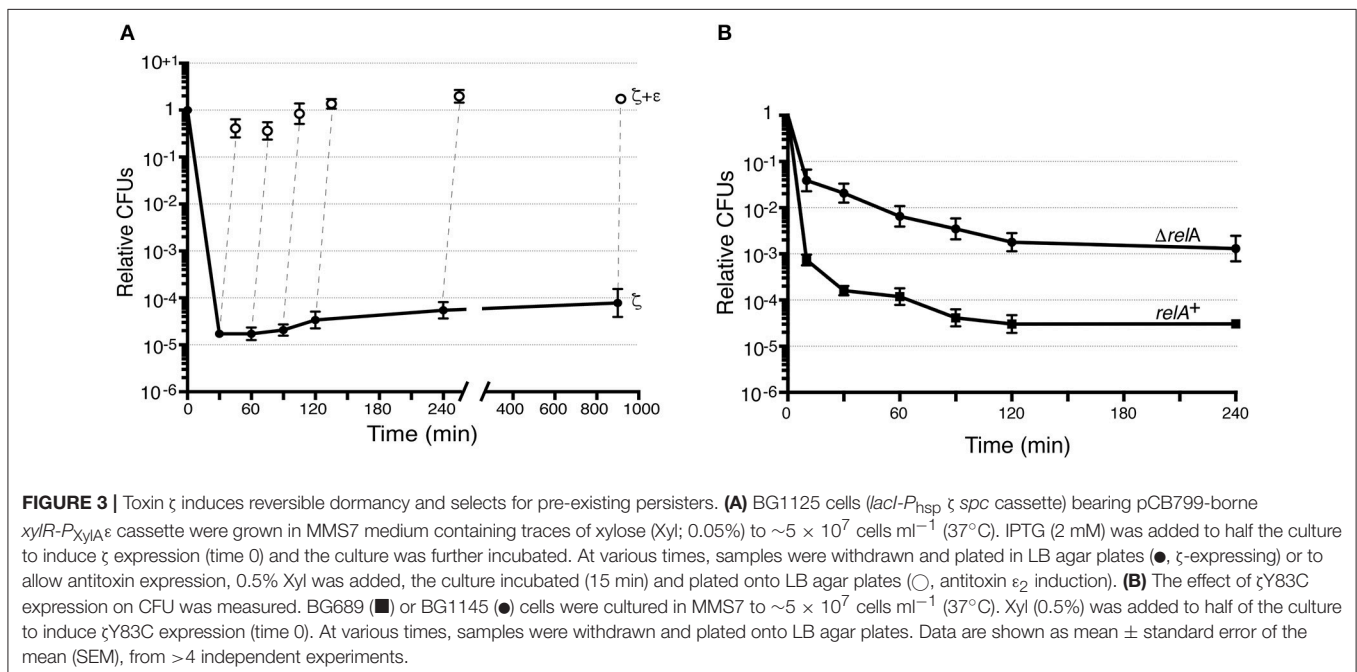
To test whether the persisters are due to noise that causes instability in a bacterial population (a reduced cell fraction transiently insensitive to toxin action) or noisy gene expression (a reduced fraction with no toxin expression), we maintained IPTG induction up to 900 min, after which cells were plated in the absence of the inducer. In the former case, only a

fraction of the non-replicating dormant cells would exit the arrest state and resume growth after plating without IPTG, whereas in the latter case, cell proliferation of persisters is predicted to increase 8- to 16-fold. After IPTG addition, the small persister subpopulation increased slightly ( $\sim 3$ -fold) during the first 240 min, to later remain apparently constant (**Figure 3A**); this suggested negligible biological noise during the first 240 min, and persisters were transiently insensitive to toxin action.

Massive expression of toxin PezT or  $\zeta$  triggers an irreversible bactericidal effect in *E. coli* grown in rich medium or *B. subtilis* grown in minimal medium, respectively (Zielenkiewicz and Ceglowski, 2005; Mutschler et al., 2011), but physiological concentrations of free toxin  $\zeta$  induce a reversible bacteriostatic state (Lioy et al., 2012). To identify the source of these discrepancies, we tested whether IPTG-induced growth arrest in *B. subtilis* cells is fully reversible after antitoxin  $\varepsilon_2$  expression triggered by 0.5% Xyl (15 min), followed by plating in LB agar with 0.5% Xyl but lacking IPTG. Antitoxin  $\varepsilon_2$  expression was sufficient to reverse growth arrest, and most cells recovered proliferation, even after 900 min of toxin  $\zeta$  action (**Figure 3A**). Although, a reduced fraction (10 to 15% of total cells) were stained with propidium iodide, suggesting a membrane compromise in these cells. It is likely that toxin  $\zeta$  induces a reversible inhibition of cell growth, and that antitoxin  $\varepsilon_2$  expression is necessary and sufficient to switch off toxin-induced responses, with cells awakening and forming colonies even after 15 h of toxin incubation (see **Figure 1**, solid red line), but 10 to 15% of total cells might loss cell viability.

## Dysregulated (p)ppGpp Levels Increase the Rate of $\zeta$ Y83C Persisters

*Bacillus subtilis* encodes one bifunctional RelA synthase-hydrolase and two mono-functional SasA (also termed



YwaC/RelP/Sas1) and SasB (YjbM/RelQ/Sas2) synthases [see Nanamiya et al., 2008; Srivatsan and Wang, 2008]. In the absence of RelA, an excess of GTP over GDP as well as baseline levels of (p)ppGpp “dysregulated” by the SasA and SasB synthases, increase toxin persistence or tolerance by >150-fold (Tabone et al., 2014b). This effect correlates with dysregulated (p)ppGpp levels. Lowering the GTP levels without affecting (p)ppGpp, by treating cells with decoyinine (a GMP synthetase inhibitor), the persistent rate was indistinguishable between treated or untreated  $\Delta relA$  cells (Lioy et al., 2012).

To test whether the CFU increase correlates with a simple decay curve predicted from a uniform tolerant bacterial population or with a biphasic time-inactivation curve due to persistence (Figure 1), we analyzed toxin expression in the  $relA^+$  (BG689) or  $\Delta relA$  (BG1145) cells bearing the  $xylR-P_{xylA}$   $\zeta Y83C$  cassette (Table 1). The  $relA^+$  and  $\Delta relA$  cells were grown in MMS7 to  $\sim 5 \times 10^7$  ml<sup>-1</sup>, expression of the  $\zeta Y83C$  gene was induced with 0.5% Xyl, and the time-inactivation curve was analyzed. In the absence of RelA, a typical biphasic curve was observed upon expression of physiological concentrations of the toxin, with an  $\sim 160$ -fold ( $\sim 5 \times 10^{-3}$ ) increase in the rate of persisters after plating on LB agar without Xyl (Figure 3B).

## Varying the c-di-AMP Pool Alters the Rate of Toxin But Not of Amp Persistence

The second messenger c-di-AMP, which is at the heart of cell wall homeostasis, is produced mainly by Gram-positive bacteria of the phyla Firmicutes and Actinobacteria, and by some species of the  $\delta$ -Proteobacteria class (Corrigan and Grundling, 2013). In Firmicutes, high or low c-di-AMP levels indirectly increase (p)ppGpp (Rao et al., 2010; Corrigan et al., 2015), whereas in *Staphylococcus aureus*, they, respectively, increase or decrease  $\beta$ -lactam tolerance/resistance (Corrigan et al., 2011, 2015). It is not known whether c-di-AMP has a role in toxin  $\zeta$  responses to stress.

In Firmicutes, intracellular c-di-AMP levels are precisely regulated by two sets of enzymes with opposite effects and by two purine nucleotides. The diadenylate cyclases (DAC) synthesize c-di-AMP from two ATP molecules, the phosphodiesterases (PDE) degrade c-di-AMP into pApA; (p)ppGpp and pApA inhibit PDE enzyme activity (Rao et al., 2010; Corrigan and Grundling, 2013; Huynh and Woodward, 2016), which predicts that c-di-AMP levels increase during starvation. Exponentially growing *B. subtilis* cells express two DAC (DisA and CdaA) and two PDE enzymes (GdpP and PgpH; Rao et al., 2010; Corrigan et al., 2011; Corrigan and Grundling, 2013; Commichau et al., 2015; Huynh and Woodward, 2016). The absence of both DAC or of both PDE causes aberrant physiology and synthetic lethality when the medium contained high K<sup>+</sup> (5 mM KCl), but one representative of each family can be deleted with no apparent effect (Corrigan et al., 2011; Corrigan and Grundling, 2013; Commichau et al., 2015; Huynh and Woodward, 2016; Gundlach et al., 2017). C-di-AMP levels vary marginally (2- to 3-fold) in cells lacking DisA, CdaA or GdpP compared to the *wt* strain (Oppenheimer-Shaanan et al., 2011; Gándara and Alonso, 2015).

To determine how *B. subtilis* cells respond to toxin-mediated stress, we induced transient toxin  $\zeta Y83C$  expression and studied

the effect of disturbing the c-di-AMP metabolic balance by deleting one DAC (DisA) or one PDE (GdpP) enzyme on an isogenic background (Table 1). In parallel, Amp was used as a second stressor at twice the MIC, in anticipation that toxin expression and Amp would respond to different physiological cues. The MIC of Amp was similar in all strains tested. After Amp exposure, a subpopulation of clonal cells yielded a biphasic time-kill curve (twodotted dashed line), which indicated that they persisted rather than becoming Amp-tolerant (dotted line; Figure 1). Similar biphasic curves are reported for other bacterial species after Amp exposure (Lewis, 2010; Amato et al., 2013; Brauner et al., 2016; Harms et al., 2016).

*Bacillus subtilis* cells that lack GdpP show intracellular c-di-AMP levels  $\sim 2$ -fold higher than those of the *wt* strain (Gándara and Alonso, 2015). Absence of GdpP indirectly increases (p)ppGpp pools (Gundlach et al., 2015; Zhu et al., 2016), which suggests that a small number of specific signaling nucleotides integrate and coordinate key metabolic intersections in response to variation of the intracellular c-di-AMP pool. We constructed and analyzed a strain bearing the  $xylR-P_{xylA}$   $\zeta Y83C$  cassette in the context of  $\Delta gdpP$  (Table 1). Regulated  $\zeta Y83C$  expression in the *wt* or  $\Delta gdpP$  contexts produced a typical biphasic survival curve, with an initial rapid decrease in CFU and a persistent subpopulation with a stable number of CFU (between 10 and 300 min; not shown); for direct comparison of the various strains, data at 120 min are shown (Figure 4). In the *wt* strain,  $\zeta Y83C$  expression used (p)ppGpp to mediate rapid inhibition of cell proliferation, and a cell subpopulation entered a toxin- ( $\sim 7.2 \times 10^{-5}$ ) or Amp-persistent state ( $\sim 2.1 \times 10^{-3}$ ; Figure 4), as reported (Lioy et al., 2012). In the  $\Delta gdpP$  strain, after transient toxin expression, the persistence rate decreased by  $\sim 10$ -fold ( $7 \times 10^{-6}$ ), but did not significantly affect the persistence rate after

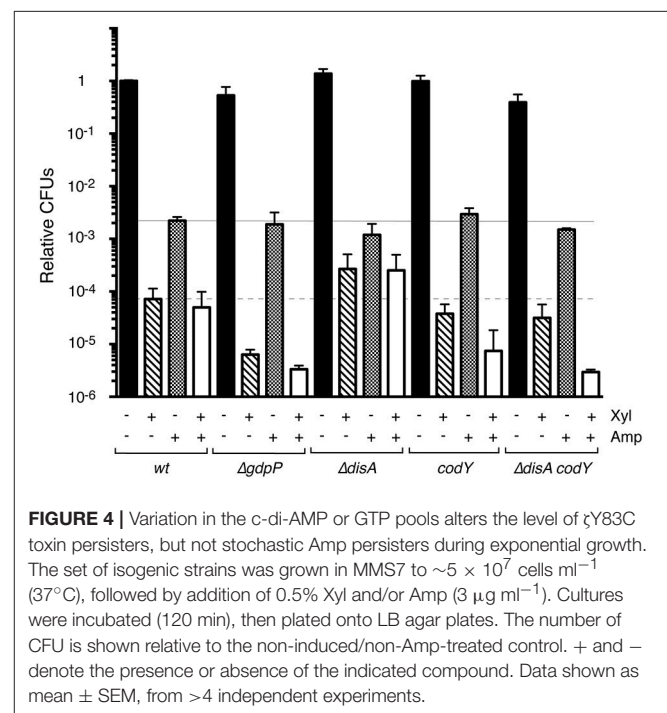


**FIGURE 4 |** Variation in the c-di-AMP or GTP pools alters the level of  $\zeta Y83C$  toxin persists, but not stochastic Amp persists during exponential growth. The set of isogenic strains was grown in MMS7 to  $\sim 5 \times 10^7$  cells ml<sup>-1</sup> (37°C), followed by addition of 0.5% Xyl and/or Amp (3  $\mu$ g ml<sup>-1</sup>). Cultures were incubated (120 min), then plated onto LB agar plates. The number of CFU is shown relative to the non-induced/non-Amp-treated control. + and - denote the presence or absence of the indicated compound. Data shown as mean  $\pm$  SEM, from >4 independent experiments.

Amp addition ( $\sim 1.7 \times 10^{-3}$ ). In the absence of GdpP, exposure to Amp and Xyl decreased the rate of persisters by  $\sim 16$ -fold ( $\sim 3 \times 10^{-6}$  survivals) compared to the *wt* strain (Figure 4), which suggests that a subset of toxin or Amp persisters randomly switched to the susceptible state and were targeted by Amp or the toxin.

Cells lacking DisA have  $\sim 2$ -fold lower levels of intracellular c-di-AMP than *wt* cells (Oppenheimer-Shaanan et al., 2011; Gándara and Alonso, 2015). We constructed the *xylR-P<sub>xylA</sub> ζY83C ΔdisA* strain (Table 1), and found that the persister cell rate was slightly affected by Amp addition ( $< 2$ -fold,  $\sim 1.5 \times 10^{-3}$  survivals). Transient toxin ζY83C expression increased persisters  $\sim 4$ -fold ( $\sim 3 \times 10^{-4}$ ) in the *ΔdisA* compared to the *wt* strain (Figure 4). Transient toxin ζY83C expression and Amp addition did not notably affect colony formation compared to addition of Xyl alone (Figure 4).

### Absence of CodY Alters the Rate of Toxin ζY83C But Not of Amp Persistence

Transient toxin ζ expression decreased the GTP pool in exponentially growing *B. subtilis* cells (Liroy et al., 2012). Intracellular GTP levels have a central role in modulating the stringent response and in reprogramming gene regulation to allow appropriate adaptation to stress. CodY, a GTP-binding protein, is a pleiotropic regulator that senses intracellular branched chain amino acids and GTP levels (Sonenshein, 2007). Low GTP levels, as found during acute stress, release CodY from DNA, leading to deregulation of genes involved in adaptation to nutrient limitation (Ratnayake-Lecamwasam et al., 2001; Belitsky and Sonenshein, 2013; Bittner et al., 2014). The role of CodY in toxin ζ stress responses is unknown. To test whether CodY modulates toxin and/or antibiotic persistence, we constructed the *xylR-P<sub>xylA</sub> ζY83C codY* strain (Table 1). Lack of CodY did not markedly alter the Amp persister rate ( $\sim 2.5 \times 10^{-3}$  survivals; Figure 4). After Xyl exposure, however, we observed a slight decrease in the toxin persister rate ( $\sim 2$ -fold) compared to *wt* cells (Figure 4). Transient Xyl and Amp addition decreased CFU ( $\sim 8 \times 10^{-6}$  survivals) and the level of persisters decreased by  $\sim 5$ -fold compared to the *wt* strain (Figure 4), which suggest that cells lacking CodY adapt poorly to toxin and Amp stress.

### Lack of CodY Suppresses Toxin Persistence Triggered by Low c-di-AMP Levels

The absence of DisA increased, and of CodY or GdpP decreased the rate of toxin persistence (Figure 4). Since lack of both CodY and GdpP strongly affected cell recovery, but the combined absence of CodY and DisA showed a less stringent phenotype, we constructed the *xylR-P<sub>xylA</sub> ζY83C ΔdisA codY* strain (BG1527; Table 1). The BG1527 strain yielded colonies with diffuse borders, a 3:1 normal:small size ratio, and viability reduced by  $\sim 1.4$ -fold compared to parental BG689 strains, but lack of CodY and DisA did not notably alter the rate of Amp persisters ( $\sim 2.5 \times 10^{-3}$  survivals). Following toxin ζY83C expression, we observed a moderate decrease ( $\sim 2$ -fold) in the toxin persister rate ( $\sim 3.5 \times 10^{-5}$  survivals) compared to *wt* cells, similar to the *codY* strain (Figure 4). Addition of Xyl and Amp greatly decreased

the persistence rate ( $\sim 3 \times 10^{-6}$  survivals; Figure 4). Different clonal subpopulations of persisting cells thus probably evolved differently in response to the toxin and Amp.

## DISCUSSION

Toxin ζ represents a class of UNAG-dependent ATPases (Figure 2A). As another mechanism to halt cell proliferation, toxin ζ also catalyzes the transfer of part of the ATP γ-phosphate generated upon ATP hydrolysis to a fraction of UNAG, to yield unreactive UNAG-3P (Mutschler et al., 2011; Tabone et al., 2014a). Stoichiometric concentrations of purified antitoxin ε<sub>2</sub> are necessary and sufficient to inactivate toxin ζ action, which suggests that no other factor contributes to ζ inactivation *in vitro*.

Using a set of isogenic *B. subtilis* strains, we tested how purine nucleotide signaling integrates and coordinates the toxin mode of action *in vivo*. Toxin ζ expression induced a biphasic time-inactivation curve with initial rapid, reversible growth arrest of the bulk of susceptible cells; a minor cell subpopulation showed non-inheritable toxin persistence rather than tolerance. Subsequent expression of the ε<sub>2</sub> antitoxin reversed ζ-induced dormancy, and the cells formed colonies even after 900 min of growth arrest. After accumulation of the ζε<sub>2</sub> complex, the heterogeneous dormancy state is nearly fully reversible; but a reduced subpopulation (up to 15%) of total cells is still stained with propidium iodide. It is likely that the ζ phosphotransferase might compromise the awakening of these cells, which may have a poor fitness or be maladapted. Persisters are formed through redundant mechanisms, and both the biological basis of persistence and the mechanisms that lead to persister formation are poorly understood in Firmicutes. Direct comparison with the well-characterized *E. coli* system could introduce some noise. For example, in both *E. coli* and *B. subtilis* cells, physiological (p)ppGpp levels are necessary for toxin-induced persistence (Korch et al., 2003; Nguyen et al., 2011; Liroy et al., 2012; Amato et al., 2013; Maisonneuve et al., 2013). In the absence of hydrolase-synthase SpoT, *E. coli* cells are not viable (Xiao et al., 1991), but in the *spoT1* context (attenuated hydrolase activity), high levels of dysregulated (p)ppGpp give rise to hypertolerance (Amato et al., 2013; Maisonneuve et al., 2013). In *B. subtilis* cells, lack of the hydrolase-synthase RelA leads to undetectable levels of dysregulated (p)ppGpp, which in turn do not inhibit GTP synthesis and contribute indirectly to hyperpersistence ( $\sim 160$ -fold increase). In the absence of (p)ppGpp, there is no persistence signal in *B. subtilis* or *S. aureus* cells, but reduction of GTP and ATP (Tabone et al., 2014b) or ATP levels (Conlon et al., 2016), respectively, leads to cell susceptibility to distinct antibiotics. Indeed, the artificial reduction of the GTP level sensitizes the cells to different antibiotics in the absence of (p)ppGpp (Tabone et al., 2014b). In *E. coli* cells that lack the 10 host-encoded mRNA interferases, levels of persisters to certain antibiotics decrease (Maisonneuve et al., 2011), whereas in *B. subtilis* cells, absence of the single mRNAase NdoA (MazF) increases antibiotic lethality rather than inducing persister cell formation (Wu et al., 2011).

A very small fraction of *E. coli* cells ( $\sim 0.01\%$ ) is reported to have a high (p)ppGpp concentration, which triggers entry into the persistent state (Maisonneuve et al., 2013). Our study



addressed the mechanism of persister formation in *B. subtilis* cells in conditions in which toxin/antitoxin expression were controlled by external inducers; antitoxin degradation thus had no role, which rendered unnecessary the analysis of (p)ppGpp in toxin release. If the stochastic switch to produce (p)ppGpp is the sole factor that triggers persister formation, the proportion of toxin and Amp persisters should be similar, and transient toxin expression and Amp addition would not further decrease cell viability. This was not observed. To explain our results, we must assume that a certain cell fraction switches stochastically to the persistent state prior to environmental challenges (Amp persisters), but sensing the metabolic state is of key importance for responsive induction of persistence. Alterations in the GTP (*codY*) or c-di-AMP pools (*gdpP* or *disA*) indicated a constant “awakening” rate after Amp addition, but a variable proportion of toxin persisters (Figure 4). Toxin  $\zeta$  temporarily and reversibly increases the (p)ppGpp pool, reduces the ATP and GTP pools, and modulates c-di-AMP and UNAG levels to allow cells to readjust their metabolism from logarithmic growth to “growth arrest,” enabling cells to cope with environmental stress. The pattern of toxin persistence was varied by altering the c-di-AMP pool, which acts as two opposite mechanisms that are negatively and positively controlled by toxin expression. The subpopulation of bet-hedging persister cells that arises before changes in the environment and those triggered by toxin-induced metabolic changes both lead to toxin persisters.

Responsive strategies based on environmental sensing alter phenotypic switching between growth-arrested and persister cells. By varying the intracellular pool of signaling nucleotide, the stochastic subpopulation of toxin  $\zeta$  persisters varied up to 40-fold ( $\Delta$ *disA* vs.  $\Delta$ *gdpP*). When both stress sources (Amp and free toxin) were present, however, a fraction of Amp (or toxin) persisters might awaken and become sensitive to the second stressor, decreasing the rate of persisters by up to 200-fold ( $\Delta$ *disA* vs.  $\Delta$ *gdpP* background).

Based on these results and our previous work (Lioy et al., 2006, 2012; Tabone et al., 2014a,b), we propose that the *modus operandi* of toxin  $\zeta$ -induced growth arrest is to reduce

the ATP (by direct hydrolysis) and GTP (by conversion to [p]ppGpp) pools. As a consequence of this, (p)ppGpp levels are increased, and a fraction of UNAG becomes phosphorylated. High (p)ppGpp directly inhibits regeneration and *de novo* GTP synthesis; it positively and negatively regulates the c-di-AMP pool, and decreases the proton-motive force (lowering the ATP pool) as well as UNAG (Kriel et al., 2012). These imbalances induce diverse transient, reversible states to ensure population survival in adverse conditions. Except (p)ppGpp dysregulation on the  $\Delta$ *relA* background, there is no direct information that a discrete metabolite increases persister formation. ATP depletion is thought to be a general mechanism of persister formation in bacteria (Conlon et al., 2016; Shan et al., 2017), although we found that a reduction in ATP levels leads to  $\zeta$ -induced growth arrest rather than to persister formation. We propose that the interrelationship between ATP, GTP, (p)ppGpp, c-di-AMP, and UNAG contribute, via a poorly characterized mechanism, to  $\zeta$ -induced cell growth arrest and persister formation.

## AUTHOR CONTRIBUTIONS

MM, VL, MT, and JA conceived and designed the experiments for this study. MM, VL, and MT performed the experiments. JA wrote the manuscript. All authors discussed the data and made comments on the manuscript.

## ACKNOWLEDGMENTS

We thank Boris R. Belitsky (Tufts University School of Medicine, Boston, MA USA) for providing the BB1043 (*codY::[erm::spc]*) mutant strain, Silvia Ayora (CNB-CSIC) for critical comments, and Catherine Mark (CNB-CSIC) for editorial assistance. MT is a PhD fellow of the La Caixa Foundation International Fellowship Programme (La Caixa/CNB). This study was supported by the Spanish Ministerio de Economía y Competitividad and the European Union (MINECO-FEDER) BFU2015-67065-P to JA.

## REFERENCES

- Amato, S. M., Orman, M. A., and Brynildsen, M. P. (2013). Metabolic control of persister formation in *Escherichia coli*. *Mol. Cell* 50, 475–487. doi: 10.1016/j.molcel.2013.04.002
- Balaban, N. Q., Gerdes, K., Lewis, K., and McKinney, J. D. (2013). A problem of persistence: still more questions than answers? *Nat. Rev. Microbiol.* 11, 587–591. doi: 10.1038/nrmicro3076
- Belitsky, B. R., and Sonenshein, A. L. (2013). Genome-wide identification of *Bacillus subtilis* CodY-binding sites at single-nucleotide resolution. *Proc. Natl. Acad. Sci. U.S.A.* 110, 7026–7031. doi: 10.1073/pnas.1300428110
- Bittner, A. N., Kriel, A., and Wang, J. D. (2014). Lowering GTP level increases survival of amino acid starvation but slows growth rate for *Bacillus subtilis* cells lacking (p)ppGpp. *J. Bacteriol.* 196, 2067–2076. doi: 10.1128/JB.01471-14
- Brauner, A., Fridman, O., Gefen, O., and Balaban, N. Q. (2016). Distinguishing between resistance, tolerance and persistence to antibiotic treatment. *Nat. Rev. Microbiol.* 14, 320–330. doi: 10.1038/nrmicro.2016.34
- Brinsmade, S. R., Alexander, E. L., Livny, J., Stettner, A. I., Segre, D., Rhee, K. Y., et al. (2014). Hierarchical expression of genes controlled by the *Bacillus subtilis* global regulatory protein CodY. *Proc. Natl. Acad. Sci. U.S.A.* 111, 8227–8232. doi: 10.1073/pnas.1321308111
- Camacho, A. G., Misselwitz, R., Behlke, J., Ayora, S., Welfle, K., Meinhardt, A., et al. (2002). *In vitro* and *in vivo* stability of the  $e_2\zeta_2$  protein complex of the broad host-range *Streptococcus pyogenes* pSM19035 addiction system. *Biol. Chem.* 383, 1701–1713. doi: 10.1515/bc.2002.191
- Carrasco, B., Yadav, T., Serrano, E., and Alonso, J. C. (2015). *Bacillus subtilis* RecO and SsbA are crucial for RecA-mediated recombinational DNA repair. *Nucleic Acids Res.* 43, 5984–5997. doi: 10.1093/nar/gkv545
- Ceglowski, P., Boitsov, A., Chai, S., and Alonso, J. C. (1993). Analysis of the stabilization system of pSM19035-derived plasmid pBT233 in *Bacillus subtilis*. *Gene* 136, 1–12. doi: 10.1016/0378-1119(93)90441-5
- Commichau, F. M., Dickmanns, A., Gundlach, J., Ficner, R., and Stulke, J. (2015). A jack of all trades: the multiple roles of the unique essential second messenger cyclic di-AMP. *Mol. Microbiol.* 97, 189–204. doi: 10.1111/mmi.13026
- Conlon, B. P., Rowe, S. E., Gandt, A. B., Nuxoll, A. S., Donegan, N. P., Zalis, E. A., et al. (2016). Persister formation in *Staphylococcus aureus* is associated with ATP depletion. *Nat. Microbiol.* 1, 16051. doi: 10.1038/nrmicrobiol.2016.51

- Corrigan, R. M., Abbott, J. C., Burhenne, H., Kaever, V., and Grundling, A. (2011). c-di-AMP is a new second messenger in *Staphylococcus aureus* with a role in controlling cell size and envelope stress. *PLoS Pathog.* 7:e1002217. doi: 10.1371/journal.ppat.1002217
- Corrigan, R. M., Bellows, L. E., Wood, A., and Grundling, A. (2016). ppGpp negatively impacts ribosome assembly affecting growth and antimicrobial tolerance in Gram-positive bacteria. *Proc. Natl. Acad. Sci. U.S.A.* 113, E1710–E1719. doi: 10.1073/pnas.1522179113
- Corrigan, R. M., Bowman, L., Willis, A. R., Kaever, V., and Grundling, A. (2015). Cross-talk between two nucleotide-signaling pathways in *Staphylococcus aureus*. *J. Biol. Chem.* 290, 5826–5839. doi: 10.1074/jbc.M114.598300
- Corrigan, R. M., and Grundling, A. (2013). Cyclic di-AMP: another second messenger enters the fray. *Nat. Rev. Microbiol.* 11, 513–524. doi: 10.1038/nrmicro3069
- De La Cruz, E. M., Sweeney, H. L., and Ostap, E. M. (2000). ADP inhibition of myosin V ATPase activity. *Biophys. J.* 79, 1524–1529. doi: 10.1016/S0006-3495(00)76403-4
- Eymann, C., Homuth, G., Scharf, C., and Hecker, M. (2002). *Bacillus subtilis* functional genomics: global characterization of the stringent response by proteome and transcriptome analysis. *J. Bacteriol.* 184, 2500–2520. doi: 10.1128/JB.184.9.2500-2520.2002
- Gándara, C., and Alonso, J. C. (2015). DisA and c-di-AMP act at the intersection between DNA-damage response and stress homeostasis in exponentially growing *Bacillus subtilis* cells. *DNA Repair* 27, 1–8. doi: 10.1016/j.dnarep.2014.12.007
- Gerdes, K. (2013). *Prokaryotic Toxin-antitoxins*. Berlin: Springer. doi: 10.1007/978-3-642-33253-1
- Gundlach, J., Herzberg, C., Kaever, V., Gunka, K., Hoffmann, T., Weiss, M., et al. (2017). Control of potassium homeostasis is an essential function of the second messenger cyclic di-AMP in *Bacillus subtilis*. *Sci. Signal.* 10:eal3011. doi: 10.1126/scisignal.aal3011
- Gundlach, J., Mehne, F. M., Herzberg, C., Kampf, J., Valerius, O., Kaever, V., et al. (2015). An essential poison: synthesis and degradation of cyclic Di-AMP in *Bacillus subtilis*. *J. Bacteriol.* 197, 3265–3274. doi: 10.1128/JB.00564-15
- Hahn, J., Tanner, A. W., Carabetta, V. J., Cristea, I. M., and Dubnau, D. (2015). ComGA-RelA interaction and persistence in the *Bacillus subtilis* K-State. *Mol. Microbiol.* 97, 454–471. doi: 10.1111/mmi.13040
- Handke, L. D., Shivers, R. P., and Sonenshein, A. L. (2008). Interaction of *Bacillus subtilis* CodY with GTP. *J. Bacteriol.* 190, 798–806. doi: 10.1128/JB.01115-07
- Harms, A., Maisonneuve, E., and Gerdes, K. (2016). Mechanisms of bacterial persistence during stress and antibiotic exposure. *Science* 354:aaf4268. doi: 10.1126/science.aaf4268
- Huynh, T. N., and Woodward, J. J. (2016). Too much of a good thing: regulated depletion of c-di-AMP in the bacterial cytoplasm. *Curr. Op. Microbiol.* 30, 22–29. doi: 10.1016/j.mib.2015.12.007
- Khoo, S. K., Loll, B., Chan, W. T., Shoeman, R. L., Ngoo, L., Yeo, C. C., et al. (2007). Molecular and structural characterization of the PezAT chromosomal toxin-antitoxin system of the human pathogen *Streptococcus pneumoniae*. *J. Biol. Chem.* 282, 19606–19618. doi: 10.1074/jbc.M701703200
- Korch, S. B., Henderson, T. A., and Hill, T. M. (2003). Characterization of the hipA7 allele of *Escherichia coli* and evidence that high persistence is governed by (p)ppGpp synthesis. *Mol. Microbiol.* 50, 1199–1213. doi: 10.1046/j.1365-2958.2003.03779.x
- Krasny, L., and Gourse, R. L. (2004). An alternative strategy for bacterial ribosome synthesis: *Bacillus subtilis* rRNA transcription regulation. *EMBO J.* 23, 4473–4483. doi: 10.1038/sj.emboj.7600423
- Kriel, A., Bittner, A. N., Kim, S. H., Liu, K., Tehranchi, A. K., Zou, W. Y., et al. (2012). Direct regulation of GTP homeostasis by (p)ppGpp: a critical component of viability and stress resistance. *Mol. Cell* 48, 231–241. doi: 10.1016/j.molcel.2012.08.009
- Leplae, R., Geeraerts, D., Hallez, R., Guglielmini, J., Dreze, P., and Van Melderen, L. (2011). Diversity of bacterial type II toxin-antitoxin systems: a comprehensive search and functional analysis of novel families. *Nucleic Acids Res.* 39, 5513–5525. doi: 10.1093/nar/gkr131
- Lewis, K. (2010). Persister cells. *Annu. Rev. Microbiol.* 64, 357–372. doi: 10.1146/annurev.micro.112408.134306
- Lioy, V. S., Machon, C., Tabone, M., Gonzalez-Pastor, J. E., Dauglavicius, R., Ayora, S., et al. (2012). The  $\zeta$  toxin induces a set of protective responses and dormancy. *PLoS ONE* 7:e30282. doi: 10.1371/journal.pone.0030282
- Lioy, V. S., Martin, M. T., Camacho, A. G., Lurz, R., Antelmann, H., Hecker, M., et al. (2006). pSM19035-encoded  $\zeta$  toxin induces stasis followed by death in a subpopulation of cells. *Microbiology* 152, 2365–2379. doi: 10.1099/mic.0.28950-0
- Lioy, V. S., Rey, O., Balsa, D., Pellicer, T., and Alonso, J. C. (2010). A toxin-antitoxin module as a target for antimicrobial development. *Plasmid* 63, 31–39. doi: 10.1016/j.plasmid.2009.09.005
- Liu, K., Bittner, A. N., and Wang, J. D. (2015). Diversity in (p)ppGpp metabolism and effectors. *Curr. Op. Microbiol.* 24, 72–79. doi: 10.1016/j.mib.2015.01.012
- Lopez, J. M., Dromerick, A., and Freese, E. (1981). Response of guanosine 5'-triphosphate concentration to nutritional changes and its significance for *Bacillus subtilis* sporulation. *J. Bacteriol.* 146, 605–613.
- Lopez, J. M., Marks, C. L., and Freese, E. (1979). The decrease of guanine nucleotides initiates sporulation of *Bacillus subtilis*. *Biochim. Biophys. Acta* 587, 238–252. doi: 10.1016/0304-4165(79)90357-X
- Maisonneuve, E., Castro-Camargo, M., and Gerdes, K. (2013). (p)ppGpp controls bacterial persistence by stochastic induction of toxin-antitoxin activity. *Cell* 154, 1140–1150. doi: 10.1016/j.cell.2013.07.048
- Maisonneuve, E., Shakespeare, L. J., Jorgensen, M. G., and Gerdes, K. (2011). Bacterial persistence by RNA endonucleases. *Proc. Natl. Acad. Sci. U.S.A.* 108, 13206–13211. doi: 10.1073/pnas.1100186108
- Meinhart, A., Alings, C., Strater, N., Camacho, A. G., Alonso, J. C., and Saenger, W. (2001). Crystallization and preliminary X-ray diffraction studies of the  $e\zeta$  addition system encoded by *Streptococcus pyogenes* plasmid pSM19035. *Acta Crystallogr. D Biol. Crystallogr.* 57, 745–747. doi: 10.1107/S0907444901004176
- Meinhart, A., Alonso, J. C., Strater, N., and Saenger, W. (2003). Crystal structure of the plasmid maintenance system  $e\zeta$ : functional mechanism of toxin  $\zeta$  and inactivation by  $e_2\zeta_2$  complex formation. *Proc. Natl. Acad. Sci. U.S.A.* 100, 1661–1666. doi: 10.1073/pnas.0434325100
- Mutschler, H., Gebhardt, M., Shoeman, R. L., and Meinhart, A. (2011). A novel mechanism of programmed cell death in bacteria by toxin-antitoxin systems corrupts peptidoglycan synthesis. *PLoS Biol.* 9:e1001033. doi: 10.1371/journal.pbio.1001033
- Mutschler, H., and Meinhart, A. (2013). Type II Toxin-Antitoxin Loci: The  $e\zeta$  Family.” in *Prokaryotic Toxin-Antitoxins*, ed K. Gerdes (Berlin; Heidelberg: Springer-Verlag), 205–223.
- Nanamiya, H., Kasai, K., Nozawa, A., Yun, C. S., Narisawa, T., Murakami, K., et al. (2008). Identification and functional analysis of novel (p)ppGpp synthetase genes in *Bacillus subtilis*. *Mol. Microbiol.* 67, 291–304. doi: 10.1111/j.1365-2958.2007.06018.x
- Nguyen, D., Joshi-Datar, A., Lepine, F., Bauerle, E., Olakanmi, O., Beer, K., et al. (2011). Active starvation responses mediate antibiotic tolerance in biofilms and nutrient-limited bacteria. *Science* 334, 982–986. doi: 10.1126/science.1211037
- Oppenheimer-Shaan, Y., Wexselblatt, E., Katzhendler, J., Yavin, E., and Ben-Yehuda, S. (2011). c-di-AMP reports DNA integrity during sporulation in *Bacillus subtilis*. *EMBO Rep.* 12, 594–601. doi: 10.1038/embor.2011.77
- Pedley, A. M., and Benkovic, S. J. (2017). A new view into the regulation of purine metabolism: the purinosome. *Trends Biochem. Sci.* 42, 141–154. doi: 10.1016/j.tibs.2016.09.009
- Potrykus, K., and Cashel, M. (2008). (p)ppGpp: still magical? *Annu. Rev. Microbiol.* 62, 35–51. doi: 10.1146/annurev.micro.62.081307.162903
- Rao, F., See, R. Y., Zhang, D., Toh, D. C., Ji, Q., and Liang, Z. X. (2010). YybT is a signaling protein that contains a cyclic dinucleotide phosphodiesterase domain and a GGDEF domain with ATPase activity. *J. Biol. Chem.* 285, 473–482. doi: 10.1074/jbc.M109.040238
- Ratnayake-Lecamwasam, M., Serrero, P., Wong, K. W., and Sonenshein, A. L. (2001). *Bacillus subtilis* CodY represses early-stationary-phase genes by sensing GTP levels. *Genes Dev.* 15, 1093–1103. doi: 10.1101/gad.874201
- Shan, Y., Brown Gandt, A., Rowe, S. E., Deisinger, J. P., Conlon, B. P., and Lewis, K. (2017). ATP-dependent persister formation in *Escherichia coli*. *MBio* 8, e02267–e02216. doi: 10.1128/mbio.02267-16
- Soldo, B., Scotti, C., Karamata, D., and Lazarevic, V. (2003). The *Bacillus subtilis* Gne (GneA, GalE) protein can catalyze UDP-glucose as

- well as UDP-N-acetylglucosamine 4-epimerisation. *Gene* 319, 65–69. doi: 10.1016/S0378-1119(03)00793-5
- Sonenshein, A. L. (2007). Control of key metabolic intersections in *Bacillus subtilis*. *Nat. Rev. Microbiol.* 5, 917–927. doi: 10.1038/nrmicro1772
- Srivatsan, A., and Wang, J. D. (2008). Control of bacterial transcription, translation and replication by (p)ppGpp. *Curr. Op. Microbiol.* 11, 100–105. doi: 10.1016/j.mib.2008.02.001
- Tabone, M., Ayora, S., and Alonso, J. C. (2014a). Toxin  $\zeta$  reversible induces dormancy and reduces the UDP-N-acetylglucosamine pool as one of the protective responses to cope with stress. *Toxins (Basel)* 6, 2787–2803. doi: 10.3390/toxins6092787
- Tabone, M., Liroy, V. S., Ayora, S., Machon, C., and Alonso, J. C. (2014b). Role of toxin  $\zeta$  and starvation responses in the sensitivity to antimicrobials. *PLoS ONE* 9:e86615. doi: 10.1371/journal.pone.0086615
- Unterholzner, S. J., Poppenberger, B., and Rozhon, W. (2013). Toxin-antitoxin systems: biology, identification, and application. *Mob. Genet. Elements* 3:e26219. doi: 10.4161/mge.26219
- Wang, J. D., Sanders, G. M., and Grossman, A. D. (2007). Nutritional control of elongation of DNA replication by (p)ppGpp. *Cell* 128, 865–875. doi: 10.1016/j.cell.2006.12.043
- Witte, G., Hartung, S., Buttner, K., and Hopfner, K. P. (2008). Structural biochemistry of a bacterial checkpoint protein reveals diadenylate cyclase activity regulated by DNA recombination intermediates. *Mol. Cell* 30, 167–178. doi: 10.1016/j.molcel.2008.02.020
- Wu, X., Wang, X., Drlaca, K., and Zhao, X. (2011). A toxin-antitoxin module in *Bacillus subtilis* can both mitigate and amplify effects of lethal stress. *PLoS ONE* 6:e23909. doi: 10.1371/journal.pone.0023909
- Xiao, H., Kalman, M., Ikehara, K., Zemel, S., Glaser, G., and Cashel, M. (1991). Residual guanosine 3',5'-bispyrophosphate synthetic activity of *relA* null mutants can be eliminated by *spoT* null mutations. *J. Biol. Chem.* 266, 5980–5990.
- Yadav, T., Carrasco, B., Myers, A. R., George, N. P., Keck, J. L., and Alonso, J. C. (2012). Genetic recombination in *Bacillus subtilis*: a division of labor between two single-strand DNA-binding proteins. *Nucleic Acids Res.* 40, 5546–5559. doi: 10.1093/nar/gks173
- Yadav, T., Carrasco, B., Serrano, E., and Alonso, J. C. (2014). Roles of *Bacillus subtilis* DprA and SsbA in RecA-mediated genetic recombination. *J. Biol. Chem.* 289, 27640–27652. doi: 10.1074/jbc.M114.577924
- Yamaguchi, Y., Park, J. H., and Inouye, M. (2011). Toxin-antitoxin systems in bacteria and archaea. *Annu. Rev. Genet.* 45, 61–79. doi: 10.1146/annurev-genet-110410-132412
- Zhu, Y., Pham, T. H., Nhiep, T. H., Vu, N. M., Marcellin, E., Chakrabortti, A., et al. (2016). Cyclic-di-AMP synthesis by the diadenylate cyclase CdaA is modulated by the peptidoglycan biosynthesis enzyme GlmM in *Lactococcus lactis*. *Mol. Microbiol.* 99, 1015–1027. doi: 10.1111/mmi.13281
- Zielenkiewicz, U., and Ceglowski, P. (2005). The toxin-antitoxin system of the streptococcal plasmid pSM19035. *J. Bacteriol.* 187, 6094–6105. doi: 10.1128/JB.187.17.6094-6105.2005

**Conflict of Interest Statement:** The authors declare that the research was conducted in the absence of any commercial or financial relationships that could be construed as a potential conflict of interest.

The reviewer RDO and handling Editor declared their shared affiliation, and the handling Editor states that the process nevertheless met the standards of a fair and objective review.

Copyright © 2017 Moreno-del Álamo, Tabone, Liroy and Alonso. This is an open-access article distributed under the terms of the Creative Commons Attribution License (CC BY). The use, distribution or reproduction in other forums is permitted, provided the original author(s) or licensor are credited and that the original publication in this journal is cited, in accordance with accepted academic practice. No use, distribution or reproduction is permitted which does not comply with these terms.